

We are IntechOpen, the world's leading publisher of Open Access books Built by scientists, for scientists

6,900

Open access books available

185,000

International authors and editors

200M

Downloads

Our authors are among the

154

Countries delivered to

TOP 1%

most cited scientists

12.2%

Contributors from top 500 universities



WEB OF SCIENCE™

Selection of our books indexed in the Book Citation Index
in Web of Science™ Core Collection (BKCI)

Interested in publishing with us?
Contact book.department@intechopen.com

Numbers displayed above are based on latest data collected.
For more information visit www.intechopen.com



Non-Destructive Testing for Ageing Management of Nuclear Power Components

Gerd Dobmann
Fraunhofer-IZEP
Germany

1. Introduction

Worldwide a renaissance of the nuclear industry is obviously taken place and many countries favour nuclear power as one reliable opportunity to generate electrical energy at very low CO₂ generating rates in order to avoid the green house effect in the earth atmosphere. However, since 1986 when the Tschernobyl accident was happening, nearly nowhere new nuclear power plants were established. The People Republic of China, India and in the last decade Japan, Finland and France are the exception. In other words, existing supply chains of former manufacturers were mainly destroyed or have changed its technical application field. Furthermore, a lot of technical expertise was lost as younger generations were influenced politically to find its interest in other scientific areas other than in nuclear physics or nuclear engineering.

Even if we can observe today a change in mind in many countries concerning the acceptance of nuclear power the question seriously is to answer: Will we find enough well skilled technicians to reliably build all the planned nuclear power plants in the future?

Therefore, life extension of existing plants the more plays an important role. This is truer as we have learnt in the last decades how many potential we have for life time extension even if we take into account ageing phenomena concerning the materials as thermal ageing, fatigue and neutron embrittlement when we think at steel components in the primary circuit; as there are the reactor pressure vessel, heat exchangers, surge line, pressurizer vessel, main cooling pumps and pipe lines. However, as in different countries life extension to an over all life time of 80 years is in discussion in future we have to take into account the infrastructure, i.e. bridges nearby, important for fluid traffic, emergency current generators, the concrete components of the containment and the cooling towers but also ageing phenomena of electric cable insulation, etc.

Within these life time extension strategies the methodology of a continuously applied ageing management worldwide is seen as an important measure to guarantee nuclear safety. Besides the application of standardised non-destructive testing (NDT) technology during inservice inspection trials in order to perform a diagnosis of the material states on-line structural health monitoring of components by enhanced and intelligent NDT-sensors and sensor-networks will play a forthcoming future role.

In Germany actually code-accepted procedures to perform ageing management were finally discussed and approved by the authorities. However, research and development in the last

decade in the Nuclear Safety Research Programme of the German Ministry for Economy and Technology was continuously performed in order to develop and qualify NDT-technology for characterisation of ageing phenomena.

The here presented chapter describes the objectives of this research and the final results obtained. In any case, the methodology of the micromagnetic NDT procedures was especially developed. This methodology is suitable for materials characterisation of magnetisable steels in terms of determination of mechanical properties. There are many similarities between movements of dislocations under mechanical loads and pinning of this lattice defects at vacancies, precipitates, grain and phase boundaries, contributing to the strength of the material and the movement of magnetic domains under magnetic loads, i.e. when the material is magnetised in a hysteresis loop.

The methodology of the Micromagnetic, Multiparameter, Microstructure and Stress Analysis (3MA) is discussed which on a wide basis of different diverse as well as redundant information allows the sensitive materials characterisation.

In case of a Cu-rich steel alloy precipitation hardening is discussed in combination with thermal ageing. It is shown that superimposed fatigue loads will enhance the thermal ageing effect.

Fatiguing of austenitic stainless steel under some conditions is combined with phase transformation from the face-centred-cubic (fcc) lattice to body-centred-cubic (bcc) martensitic phase which is ferromagnetic of nature. Where the carbon content is low enough to avoid the phase transformation other NDT techniques based on electric conductivity effects or ultrasonic wave propagation phenomena have to be applied.

3MA is sensitive to characterise neutron embrittlement in pressure vessel materials. Material of western pressure vessel design as well as of Russian design were characterised which shows that a new NDT technology for inservice inspection of the pressure vessel wall from the id-surface can be developed.

2. Micromagnetic properties and micromagnetic NDT, the 3MA approach

The reason to develop 3MA (Micromagnetic-, Multiparameter-, Microstructure-, and stress-Analysis) by Fraunhofer-IZFP, starting in the late seventies in the German nuclear safety program, was to find microstructure sensitive NDT techniques to characterise the quality of heat treatments, for instance the stress relieve heat treatment of a weld. George Matzkanin (Matzkanin, 1979) just has had published a NTIC report in the USA to the magnetic Barkhausen noise, nowadays very often called magnetic Barkhausen emission (MBE). The technique was sensitive to microstructure changes as well as to load-induced and residual stresses. Therefore a second direction of research started in programs of the European steel industry and the objective was to determine residual stresses in big steel forgings, like turbine shafts. Beside the magnetic Barkhausen effect a magneto-acoustic-one became popular (Theiner & Waschies, 1984). The technique has based on acoustic emission measurements during controlling the magnetisation in a hysteresis cycle but was - because of the high amplification - sensitive to electric interference noise. Therefore the acoustic Barkhausen noise technique has never found a wide-spread real industrial application. However, because influenced by only 90° Bloch-wall interactions in the laboratory the technique was an ideal sensor to enhance the basic understanding. Later, further micromagnetic techniques were developed: the incremental permeability measurement, the harmonic analysis of the magnetic tangential field and the

measurement of the dynamic or incremental magnetostriction by use of an EMAT (Altpeter, 2002). Basically the idea of Paul Höller, a former director of IZFP, was to develop the micromagnetic techniques in order to replace electron microscopy, i.e. to find algorithms to determine microstructural parameters like vacancy density and distribution, dislocation density and distribution, precipitation density and distribution, etc. However, because the need for calibration of the micromagnetic measuring parameters, the researchers very quickly understand to follow the more pragmatic direction, i.e. to directly correlate the micromagnetic properties with mechanical technological parameters like yield strength or hardness. The main argument for that decision was the large scatter in electron microscopy data and the fact of the strong propagation of errors in the calibration, when based on these data.

2.1 Micromagnetic basics

Ferromagnetic materials - even in a demagnetised or 'virgin' state - consist of small, finite regions called domains (Kneller, 1966; Seeger, 1966; Cullity, 1972; McClure & Schröder, 1976). Each domain is spontaneously magnetised to the saturation value of the material. The directions of magnetisation of the various domains, however, are such that the specimen as a whole shows no net magnetisation. The process of magnetisation is then one of converting the multi-domain state into a single domain magnetised in the same direction as the applied magnetic field H . The process is performed not continuously but stepwise by movement of the domain walls, named Bloch walls, and for stronger applied fields, by rotation of the magnetisation vectors in the domains into the direction of the applied field. In iron-based materials we find 180° and 90° Bloch walls. The indicated angle is the angle between the magnetisation vectors in two adjacent domains. Domains with directions parallel or nearly parallel to the magnetising field increase in their size while all others are annihilated. The Bloch wall movements as wall jumps take place discontinuously because the walls in a polycrystalline material are temporarily pinned by lattice defects as microstructural obstacles like dislocations, precipitates, phase- or grain-boundaries. The stepwise pull-out of the wall from the obstacle changes the magnetisation state locally and is called a Barkhausen event. The local magnetisation changes induce pulsed eddy currents in the vicinity of the events propagating in all spatial directions. The amplitudes of the eddy currents are damped according to a well known dispersion law, i.e. higher frequencies in the spectrum are damped more than lower frequencies. The eddy currents induce electrical voltage pulses, called Barkhausen noise, which may be detected by an induction coil surrounding the magnetised specimen. The time domain integral of the Barkhausen noise during a magnetisation reversal is the magnetic induction B , and B versus H is the hysteresis loop. Figure 1 documents the influence of different microstructures (ferrite / martensite) and Figure 2 presents the influence of load-induced or residual mechanical stresses. 'Magnetic hard' materials, like a martensitic steel microstructure, have larger coercivity (tangential magnetic field value H_t at $B=0$) and smaller remanence (B -value at $H_t=0$). In case of compressive stresses the hysteresis is sheared and tensile stress generates a sligher curve. Whereas the hysteresis - by definition - is measured by a coil surrounding the specimen under magnetisation, more suitable pick-up techniques for local, spatially resolved ND-testing have been developed.

Ferromagnetic materials show the property of magnetostriction (Cullity, 1972). When exposed to a magnetic field, its dimension changes. The effect can be measured as a function

of the applied magnetic field in profile-curves ($\lambda(H_t)$ or $\lambda_L(H_t)$, L-lengthwise magnetised cylindrical specimen) by using strain gages (Figure 3 and Figure 4). The inverse effect, called Villari effect, is the spontaneous magnetisation of a virgin ferromagnetic material exposed to a mechanical stress field. This is the reason of the stress sensitivity of micromagnetic NDT (Sablík, Burkhart, Kwun, & Jiles, 1988; Burkhart & Kwun, 1989; Jiles 1988). In the lower part of Figure 4, according to a 4-domain model, the effect of increasing tensile stress on the domain wall movement is discussed. The domains with magnetisation direction in the tensile stress direction are preferred.

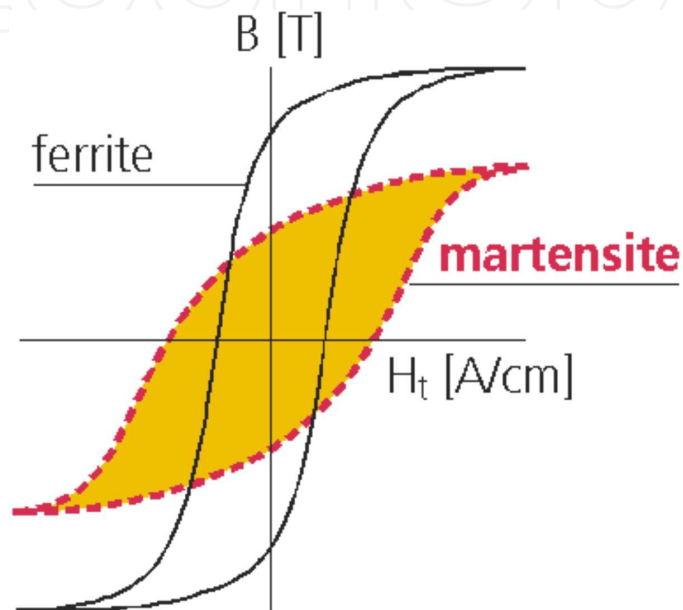


Fig. 1. Hysteresis loop and influence of microstructure

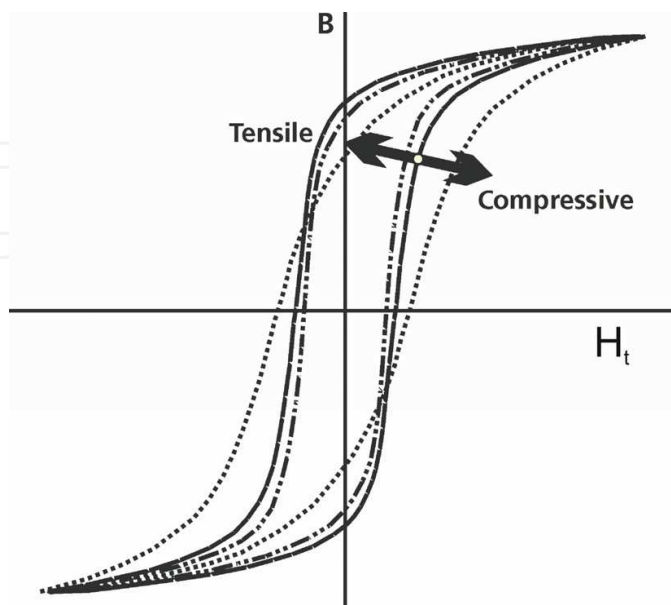


Fig. 2. Hysteresis loop and influence of mechanical stress

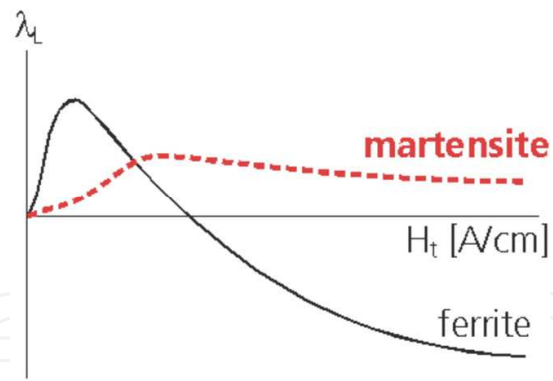


Fig. 3. Lengthwise magnetostriction and influence of microstructure

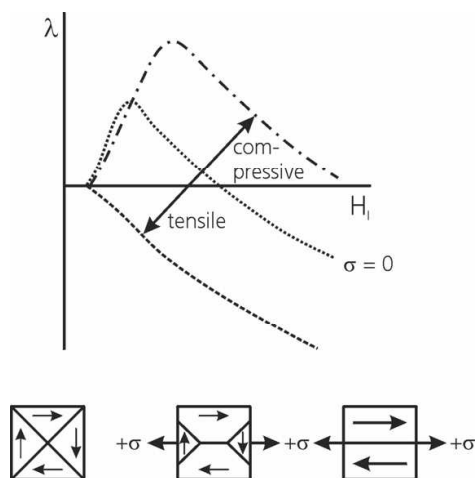


Fig. 4. Lengthwise magnetostriction and influence of mechanical stress

2.2 Micromagnetic techniques in detail

For the development of non-destructive (ND)-techniques, some special principles have been identified from the above mentioned basic physical facts, providing a selective interaction with the microstructure and stress fields. These are particularly micromagnetic techniques. Depending on the magnetic process performance irreversible and reversible processes have to be distinguished. Techniques using irreversible processes take advantage of the non-linearities of the hysteresis which are the result of the above mentioned Bloch-wall jumps and rotational processes (Jiles, 1990).

A distortion factor K can be derived from a Fourier analysis of one period of the time-signal of the magnetic tangential field strength H_t which is measured by a Hall element. K is the geometrical average (root-mean-square-value) of the power of the upper harmonics, normalised to the power of the fundamental (Pitsch, 1989). The distortion factor K is defined as shown in Figure 5. By empirical investigations it was documented that from the time dependence of the sum of all harmonics above the fundamental a coercivity value H_{C0} may be derived. This value correlates with the hysteresis coercivity H_C . The investigations are confirmed by other authors (Fillon, Lord, & Bussiere, 1990). Thus, using this measurement of the tangential field strength, with only one sensor, two independent parameters (K and H_{C0}) may be derived. The depth that is analyzed is controlled by the penetration depth of the applied field H_t .

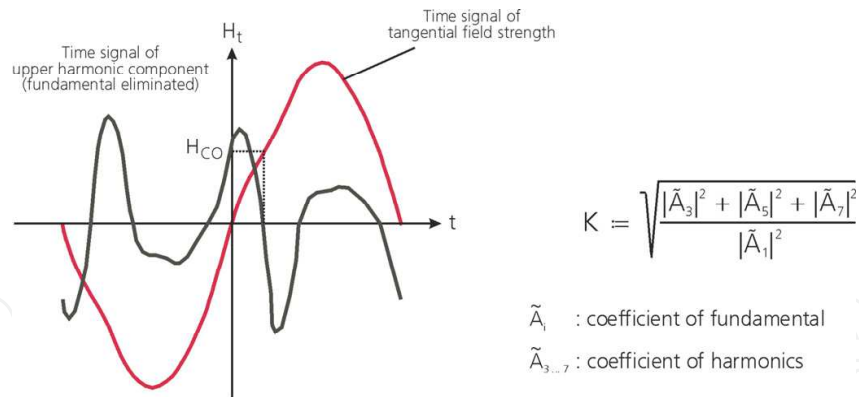


Fig. 5. Fourier analysis of the magnetic tangential field

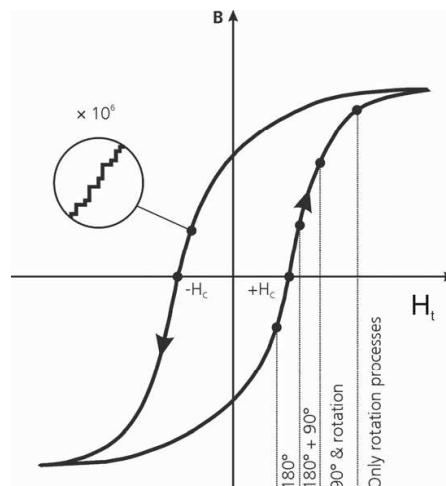


Fig. 6. Hysteresis, Barkhausen noise, micromagnetic events: Bloch wall jumps, rotation processes

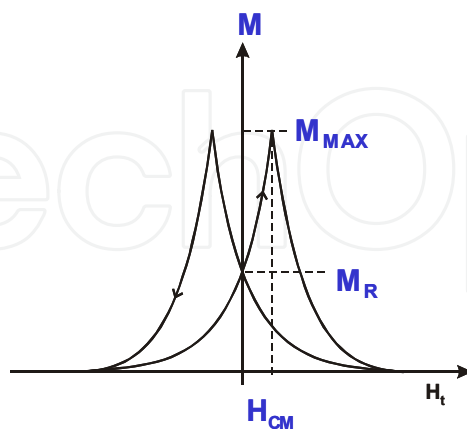


Fig. 7. Magnetic Barkhausen noise profile curve

The Barkhausen noise is magnetically received – as said before - directly by a pick-up air-coil, a ferrite-core-coil, or other inductive sensor as induced electric voltage pulses. After low-noise pre-amplification (60 dB fixed), band-pass filtering (cut-off frequencies to be adjusted), rectifying, low-pass-filtering in order to receive the envelope of the high-

frequency content of the noise, and final amplification (variable up to 60 dB), the magnetic Barkhausen noise profile-curve $M(H_t)$ is obtained (Theiner, Altpeter, & Reimringer, 1989). This type of measurement technique was proposed by Matzkanin.

The spatial resolution is restricted by the sensor geometry. The mm-range can be achieved by using standard pick-up air coils. The band pass filter is needed to suppress the large magnitude of the fundamental magnetising frequency in the received signal in addition to its higher harmonics. This effect is stronger for magnetic soft materials than for hard ones. Soft materials have an essential higher harmonic content. Harmonics up to the 7th order are observed. The lower cut-off frequency of the band pass filter therefore has to be adjustable, depending on the material under inspection. It should be mentioned here, that this measure to suppress disturbing effects and to only receive the random Barkhausen noise limits on one hand the analyzing depth for technical steels in general to a depth of ≈ 2 mm. Because on the other hand the analyzing depth of the above mentioned distortion factor measurement is limited only by the magnetising frequency, this parameter K completes the information of the Barkhausen noise to a larger analyzing depth. Because of the random character of the Barkhausen-noise a large natural scatter in the data is observed due to small magnetic fluctuations from the environment superimposed on the driving field. Time averaging (up to ten magnetising cycles) is a help to obtain reliable data. In process applications at higher inspection speeds, the effect can hinder the use of Barkhausen-noise.

Figure 6 shows a hysteresis loop as a continuous curve. Only with a higher amplification the fact of the discontinuous magnetisation in Bloch wall jumps is revealed. The Figure documents the fact of the interaction of the different Bloch-wall types at different magnetic field amplitudes. In the vicinity of the coercivity mainly the 180° walls contribute with their jumps to the magnetising process. The 90° walls need more energy for movement and therefore their contribution to magnetisation is in the knee region of the hysteresis followed by rotation processes.

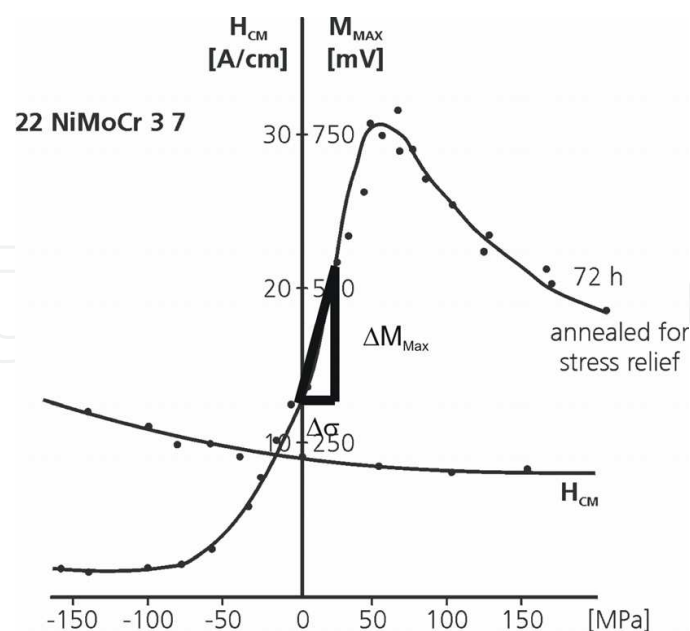


Fig. 8. Barkhausen noise peak maximum and peak separation as function of mechanical stress and stress sensitivity $\Delta M_{\text{Max}} / \Delta \sigma$ of the German pressure vessel steel 22 NiMoCr 37 after welding and 72h stress relief annealing

Fig. 7 shows a Barkhausen noise profile-curve ($M(H_t)$) and the measuring parameters are presented. For some steel grades we can observe profile-curves with up to three peaks per magnetising half-cycle, depending on the materials microstructure. Besides the different peak maxima (M_{Maxi} , $i=1, \dots, 3$) their separation (H_{CMI}) as well as different half-width-values (for instance $\Delta M_{50\%}$) are measured.

For residual stress characterisation (see Figure 8), the peak values are measured as a function of compressive and tensile stress, M_{Max} versus stress σ . The magnetic stress sensitivity of a material microstructural state is characterised by the function $\Delta M_{Max}(\sigma) / \Delta \sigma$ i.e., the inclination of the curve $M_{Max}(\sigma)$ at $\sigma = 0$. The fact of the decreasing of the peak amplitude of the Barkhausen noise at higher tensile stress levels is observed at a mechanical stress value in the tensile regime at which the magnetostriction curve under magnetisation (see Figure 4) starts directly with negative values.

Due to magnetostrictive effects, Barkhausen-events excite, in their vicinity, pulsed magnetostrictive strains which result in magnetostrictively excited acoustic emission signals named acoustic Barkhausen noise (Theiner & Waschkies, 1984). This is named as MAE – magneto-mechanical-acoustic-emission in literature too (Buttle & Hutchings, 1992; Allen & Buttle, 1992). The acoustic emission (AE) is received by narrow band, sensitive AE-transducers. Nevertheless, a high amplification of $\sim 80 - 100$ dB is needed and the technique is sensitive to disturbing noise. Typical AE-signal analysis equipments like RMS-voltmeters or energy-modules are in use. Because of its sensitivity for disturbing noise, the technique can reliably be applied only in the laboratory. Nevertheless investigations with this technique are of interest for comprehensive interpretation studies because here only the information of 90° Bloch wall movement and their interaction with the microstructure is observed.

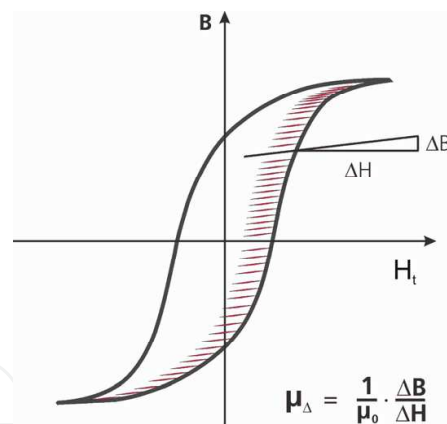


Fig. 9. Incremental permeability

Applying reversible magnetic techniques, the material is magnetised with a much smaller field strength amplitude ΔH compared to the coercivity (H_C) of the material. The magnetisation follows linearly the magnetic field. Therefore, all eddy current techniques using low electric currents in the pick-up coil, resulting in small magnetic fields ΔH ($\Delta H \ll H_C$), are reversible techniques. Parameters influencing the coil impedance are the operating frequency f_{Δ} , the electrical conductivity σ_{el} and the incremental permeability μ_{Δ} . The latter depends on the magnetic history of the specimen under inspection. An eddy current impedance spectroscopy is performed by tuning the frequency from high to low values. (σ_{el} , μ_{Δ}) - gradients in near surface zones are sensed by changing the field penetration. The spatial resolution is the same as that for eddy current coils.

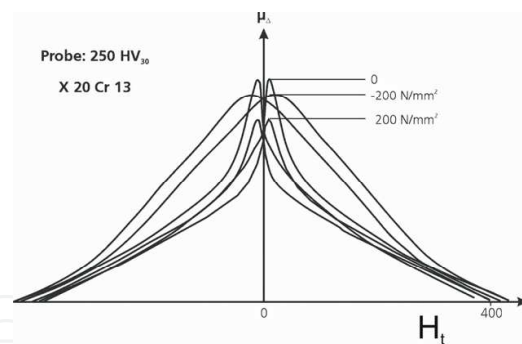


Fig. 10. Incremental permeability profile curves documenting the influence of mechanical stress, steel quality X20Cr13

The incremental permeability profile-curve, $\mu_{\Delta}(H_t)$, as a function of a controlled applied magnetic field H_t is a well defined property of the material and independent of the magnetic prehistory as long as $H_{Max} \gg H_C$ and $\Delta H \ll H_C$. The frequency f_{Δ} of the incremental field ΔH is a parameter for selecting the depth of the analyzed near surface zone; f_{Δ} should be chosen such that $f_{\Delta} \geq 100 \times f$, where f is the frequency of the applied field H_t , controlling the hysteresis. $\mu_{\Delta}(H_t)$ is measured as eddy current impedance parallel to the hysteresis reversals. The hysteresis is modulated by the alternating field ΔH , excited by the eddy current coil. The spatial resolution is the same as that for eddy current coils. Figure 9, shows the hysteresis with the inner loops, performed by the above mentioned modulation. By definition $\mu_{\Delta}(H_t)$ is proportional to the inclination of each individual inner loop touching the hysteresis for magnetic field values H_t . In Figure 10 $\mu_{\Delta}(H_t)$ profile-curves are presented, indicating the characteristic measuring parameters as function of mechanical stresses.

The dynamic or incremental magnetostriction profile-curve $E_{\lambda}(H_t)$ is the intensity of ultrasound which is excited, and received by an EMAT (Electro-Magnetic-Acoustic-Transducer) (Salzburger, 2009) for instance by measuring a back-wall echo, caused by magnetostrictive excitation as a function of the applied field H_t , controlling the hysteresis. The incremental, alternating field ΔH in this case is excited by the EMA - transmitter using a pulsed current.

The magnetostriction is modulated. (Figure 11, upper part) The spatial resolution - depending on the transmitter design - is of the order of ~ 5 mm. In order to achieve such a spatial resolution, an EMA - receiver was designed to transform the ultrasonic signal into an electrical signal only using the Lorentz-mechanisms (Koch & Höller, 1989). Figure 11, lower part, presents a half-cycle of the dynamic magnetostriction profile-curve $E_{\lambda}(H_t)$ in the magnetic field range < 300 A/cm. The amplitude value of the first peak as well as the corresponding tangential magnetic field value as well as the H_t -field position of the minimum are sensitive quantities for materials characterisation.

The micromagnetic measurements are performed by an intelligent transducer consisting of a handheld magnetic yoke together with a Hall-probe for measuring the tangential magnetic field strength and a pick-up coil for detecting the magnetic Barkhausen noise or the incremental permeability. Normally a U-shaped magnetic yoke is used, which is set onto the surface of the material under inspection, i.e. the ferromagnetic material is the magnetic 'shunt' of the magnetic circuit. Therefore all the well known design rules for magnetic circuits have to be observed. The mathematical methodology of the Micromagnetic-, Multiparameter-, Microstructure-, and stress- Analysis (3MA) in detail is described in (Altpeter, 2002). However, a short explanation is given here according to Figure 12.

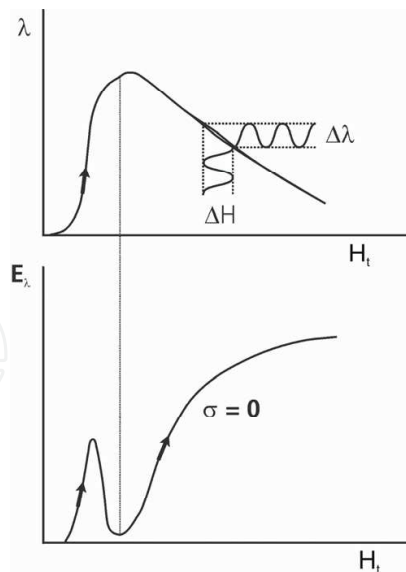


Fig. 11. Dynamic or incremental magnetostriction

With 3MA different micromagnetic quantities, let's say X_i , $i = 1, 2, 3, \dots$ are measured at 'well defined' calibration specimens. These are derived by analysis of the magnetic Barkhausen noise $M(H_t)$ and the incremental permeability $\mu_\Delta(H_t)$ as function of a tangential magnetic field H_t which is analysed and by eddy current impedance measurements at different operating frequencies.

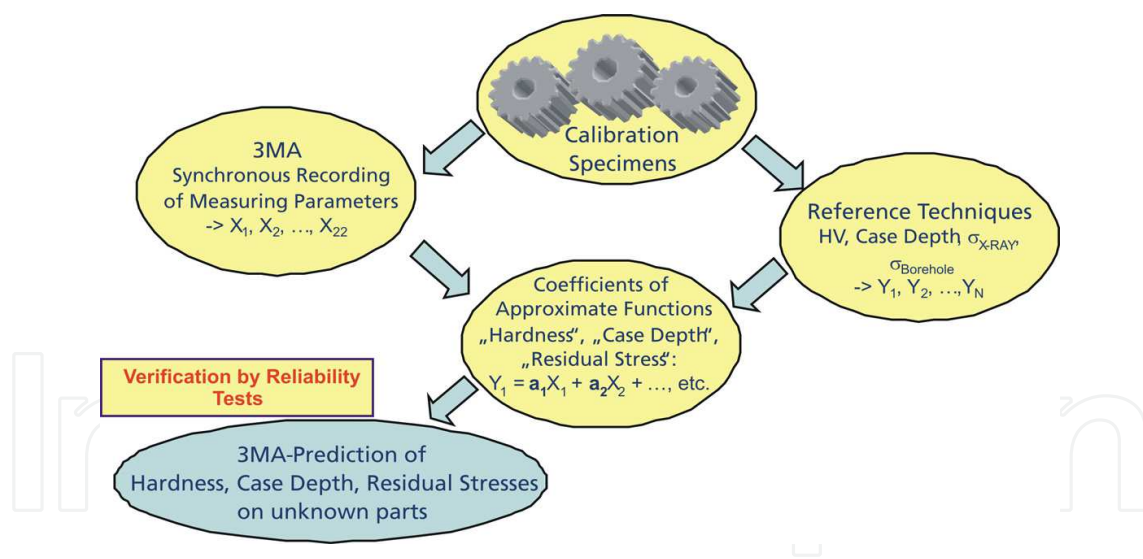


Fig. 12. The 3MA-calibration

'Well defined' here has the meaning that the calibration specimens are reliably described in reference values like mechanical hardness (according to Vickers or Brinell, etc.) or strength values like yield and/or tensile strength, or residual stress values measured, for instance, by X-ray diffraction. A model of the target function is assumed (for instance Vickers Hardness $HV(X_i)$, or strength value like $Rp0.2(X_i)$, or residual stress $\sigma_{res}(X_i)$). This model is based on the development of the target function by using a (mathematically) complete basis function system, which is a set of polynomials in the micromagnetic measurement parameters X_i . The unknown in the model are the development coefficients, in Figure 12 called a_i . These a_i are

determined in a least square or other algorithm, minimizing a norm of the residual function formed by the difference of the model function to the target reference values. In order to stochastically find a best approximation, only one part of the set of specimens is used for calibration of the model, the other independently selected part is applied to check the quality of the model (verification test). By using for instance the least square approach the unknown parameters are the solution of a system of linear equations.

3MA is especially sensitive to mechanical property determination as the relevant microstructure is governing the material behaviour under mechanical loads (strength and toughness) in a similar way as the magnetic behaviour under magnetic loads, i.e. during the magnetisation in a hysteresis loop. Because of the complexity of microstructures and the superimposed stress sensitivity there is an absolute need to develop the multiple parameter approach.

3. NDT characterisation of thermal ageing due to precipitation

Beginning in 1998 Fraunhofer-IZFP in co-operation with the Materials Testing Institute at the University Stuttgart (MPA) (Altpeter, Dobmann, Katerbau, Schick, Binkele, Kizler, & Schmauder, 1999) has investigated the low-alloy, heat-resistant steel 15 NiCuMoNb 5 (WB 36, material number 1.6368) which is used as piping and vessel material in boiling water reactor (BWR) and pressurized water reactor (PWR) nuclear power plants in Germany. One argument for its wide application is the improved 0.2% yield strength at elevated temperatures.

Conventional power plants use this material at operating temperatures of up to 450°C, whereas German nuclear power plants apply the material mainly for pipelines at operating temperatures below 300°C and in some rare cases in pressure vessels up to 340°C (e.g., a pressurizer in a PWR). Following long hours of operation (90,000 to 160,000 h) damage was seen in piping systems and in one pressure vessel of conventional power plants during the years 1987 to 1992 (Jansky, Andrä, & Albrecht, 1993) which occurred during operation and in one case during in service hydro-testing. In all damage situations, the operating temperature was between 320° and 350°C. Even though different factors played a role in causing the damage, an operation-induced hardening associated with a decrease in toughness (-20%) was seen in all cases. The latter is combined with a shift in the transition temperature of the notched-bar impact test to higher temperatures (+70°C) and in the 0.2% yield strength of about +140 MPa.

According its specification the steel has in between 0.45 and 0.85 mass% Cu (in average 0.65%) in its composition. The half part of the Cu is in precipitation because of annealing and stress relieve heat treatment during production, the other half still is in solid solution and can precipitate when the material is exposed at service temperatures. The material can obviously be recovery annealed when after the service exposures again is heated-up at the stress relieve heat treatment temperature and hold some time. The precipitates are dissolved again in solid solution obtaining a microstructure state comparable but not identical to the 'as delivered' state.

Micromagnetic investigations at first were performed at 'service exposed' (57,000h at 350°C) and 'recovery annealed' (service exposed + 3h 550°C) material using cylindrical (diameter 8mm) test specimens. Whereas the hysteresis curves of the two microstructure states are nearly identical, differences were observed when the magnetic Barkhausen noise was

registered and when the lengthwise magnetostriction was measured. The specimens were measured in the stress-free state as well under variable tensile load (according to Fig. 8) in order to reveal the stress sensitivity of the microstructures.

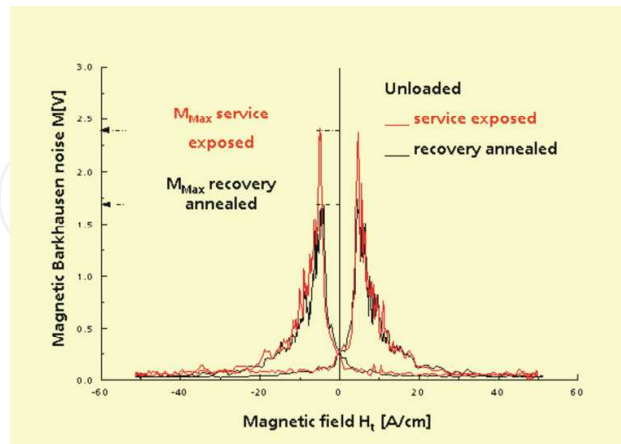


Fig. 13. Magnetic Barkhausen noise of service-exposed and recovery annealed WB36 microstructures in the stress-free state

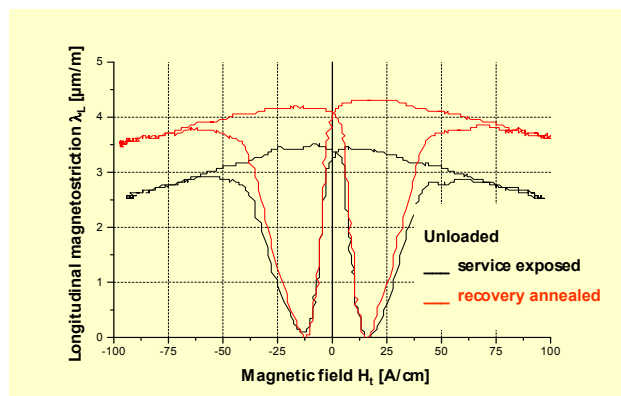


Fig. 14. The lengthwise magnetostriction of the microstructure states of Fig. 13

In Figure 13 the profile curves of the magnetic Barkhausen noise related to the two material states are shown and Figure 14 documents the behaviour of the magnetostriction in the stress-free state.

The service exposed microstructure has higher Barkhausen noise maximum and lower magnetostriction values. Both effects indicate the influence of tensile residual stresses induced by the Cu-rich precipitates in the iron matrix. In TEM and SANS investigations the precipitation state was studied. The particle size is in between 2nm – 20nm distributed. Particles < 6nm diameter have body centered cubic crystallographic structure like the iron matrix (coherent precipitates). As the atomic radius of Cu is larger compared with iron the Cu precipitate acts with compressive stresses which are balanced by tensile residual stress in the matrix. Particles with diameter > 20nm are face centered cubic and in between these two states a transition crystallographic structure exist. About 50% of the precipitates have this transition structure and especially contribute to micro residual stresses in the tensile stress regime in the matrix. Figure 15 shows the like coffee-beans shaped particles of the transition structure visible in the TEM and the diffraction pattern.

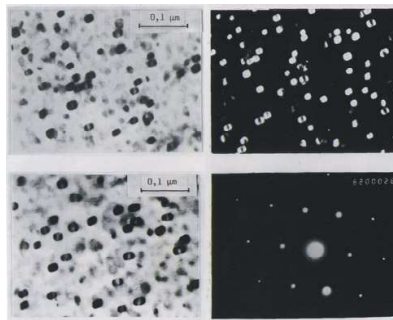


Fig. 15. TE micrographs and diffraction pattern of the Cu particles

Fraunhofer-IZFP has performed experiments under load-induced tensile stresses too. Figure 16 and Figure 17 show the result at the service exposed and recovery annealed microstructures. As discussed in Figure 8 the Barkhausen noise maximum M_{max} (σ) as function of the tensile load σ increases with the load to an absolute maximum and then decreases again. The threshold load where this maximum occurs is exactly the load value where magnetostriction becomes directly negative in sign when the specimen additionally is magnetised.

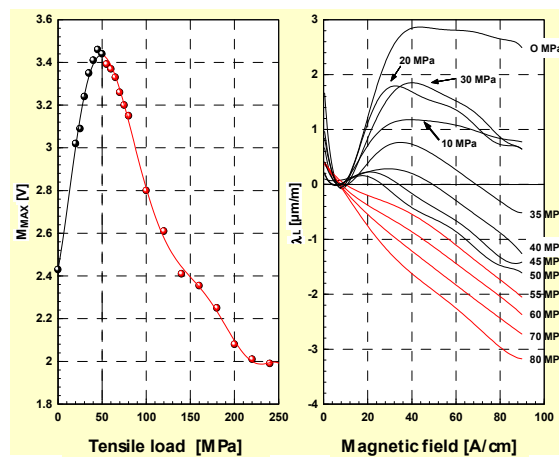


Fig. 16. The service exposed microstructure

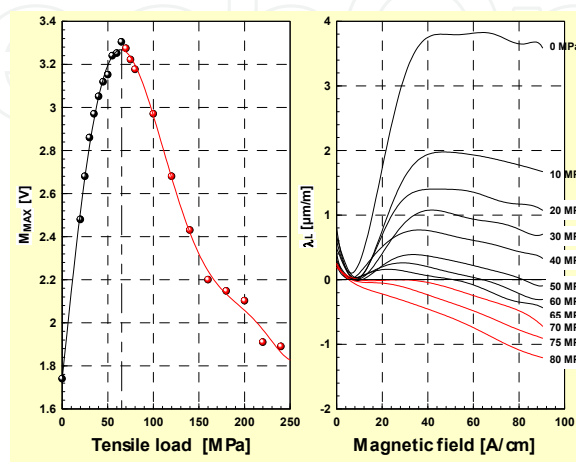


Fig. 17. The recovery annealed microstructure

Comparing the two microstructure states in its stress sensitivity the difference in the residual stress state due to the Cu precipitates can only be responsible to shift the maximum position about 17-20 MPa to smaller tensile loads in the case of the service exposed material. This value should be the amount of the average residual stress in the iron matrix which locally near the precipitate can be much higher but cannot be measured with another reference technique.

Further investigations in order to statistically confirm the results were performed at 400°C in order to speed-up the precipitation process.

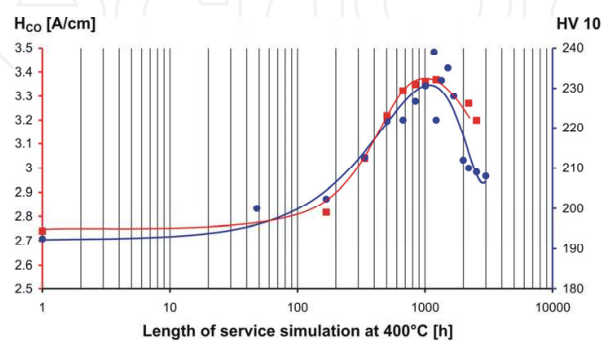


Fig. 18. Coercivity H_{C0} derived from the harmonic analysis of the tangential magnetic field strength and Vickers hardness 10

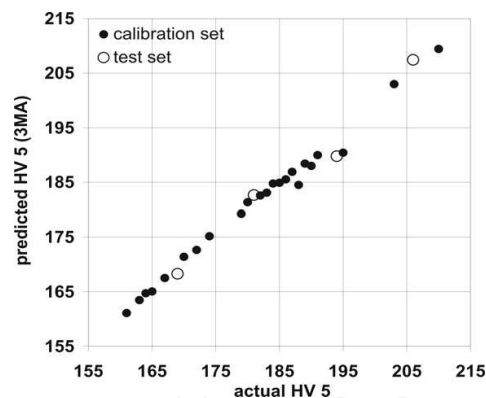


Fig. 19. 3MA approach to characterise the Cu precipitation microstructure state in terms of Vickers hardness 5

Comparing the coercivity (Figure 18.) derived from the harmonic analysis of the tangential magnetic field strength with the measured Vickers hardness 10 as reference to characterise the thermally aged microstructure both quantities are correlated and meet a typical hardness maximum which is the critical material state for possible failure of a component if the design has not taken into account the strengthening ageing effect. When the exposure times are further enlarged hardness is decreasing by precipitation coarsening. In order to obtain the good correlation in the 3MA-approach beside micromagnetic characteristics eddy current impedances were implemented. These are especially suitable as the Cu precipitates contribute to an enhanced electrical conductivity.

Parallel to the project activities in the German nuclear safety program a PhD thesis (Rabung, 2004) was performed in different projects of the German National Science Foundation (DFG). Fe-Cu-model-alloys were investigated mainly to study the effect of the Cu

precipitates without influences of the magnetic cementite-phase as in WB36. The Cu-content was varied in between 0.65% and 2.1% (Altpeter, I., Dobmann, G., Kröning, M., & Rabung, M., 2009).

There was always the supposition that any form of energy, other than only heat, put in WB36 components will contribute to enhanced precipitation of Cu particles. The effect of low cycle fatigue at service temperature was therefore studied in a further project in the German nuclear safety program the last 4 years (Altpeter, I., Szielasko, K., Dobmann, G., Ruoff, H., & Willer, D., 2010). As in literature (Solomon & De Lair, 2001) dynamic strain ageing (DSA) was expected in the lower temperature regime (200°C) to be additionally a driver for WB36 thermal degradation two different heats were selected which were different in the Al/N-ratio in the composition. Because of the higher N content (Al/N (E2)=0.92) the heat E2 was assumed to be more prone for DSA than the heat E59 (Al/N (E59)=3.87). E2 material came from a plate in the virginal condition ('as delivered state'), named E2A. The E59 material came from a used vessel which at 350°C for 57,000 h was in service. The material was investigated in the state 'recovery annealed' (600°C, 3h) named E59 EG. Furthermore, some material of E59 was especially heat treated, 'stepwise stabilised annealed' in order to stabilise the Cu precipitation distribution in coarse particles, named E59 S4. Compared with E59 EG, E59 S4 should be less prone for further precipitation development under service conditions.

Under LFF-conditions (mean strain-free, $R_{\epsilon}=-1$, strain-controlled with $\Delta\epsilon=1.05\%$ at 220°C and 300°C) specimen of the heat E2A were cycled in one-step fatigue tests with cycle period (24s, load cycles 350 at 220°C; 2400s, load cycles 200 at 220°C; 2400s, load cycles 200 at 300°C). The expected material behaviour was confirmed, i.e. degradation will be enhanced by accumulated elastic-plastic deformation; Figure 20 represents the result in terms of Charpy-test-energy versus test temperature. As documented, the 41J ductile-to-brittle transition temperature (DBTT, ΔT_{41J}) shifts to higher temperature with plastic deformation energy input.

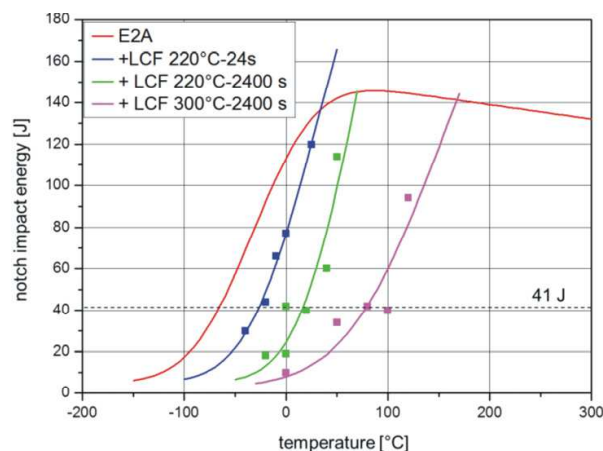


Fig. 20. Charpy tests at different thermally aged and LC fatigued material states, documentation of material degradation of the heat E2A

A maximum shift ΔT_{41J} of 144.3°C can be observed. It should be mentioned here that the tests performed with the heat E59EG have shown much smaller effects in degradation, documenting the fact that the microstructure states in the state 'as delivered' and 'recovery annealed' are not identical when exposed to further thermal ageing and fatigue.

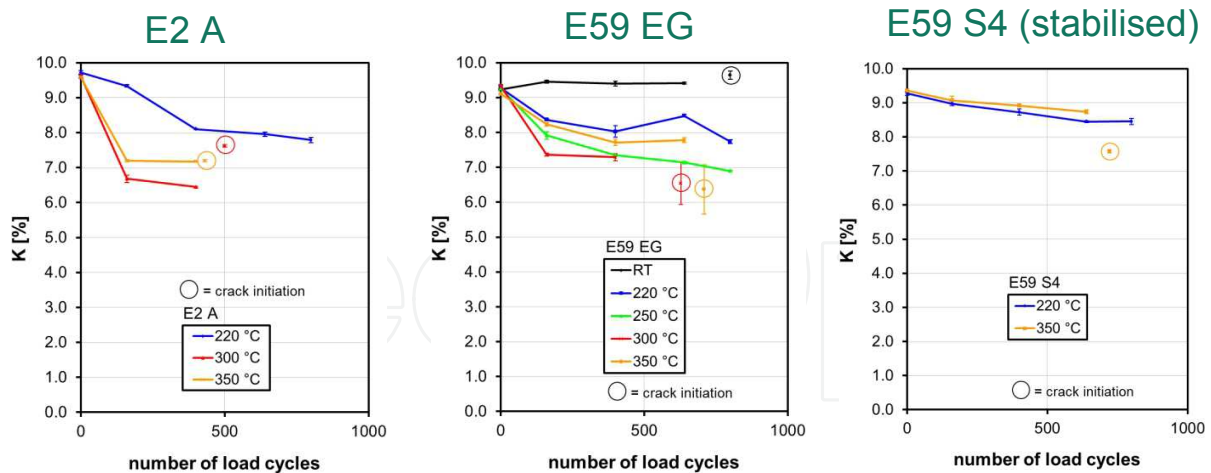


Fig. 21. Distortion factor K as function of cycle number measured after well defined fatigue intervals in test interruptions followed by a further fatiguing of the same specimen

A very wide space for investigations was addressed to interval tests where all of the 3 heats were fatigued mean strain-free with $\Delta\varepsilon=1.05\%$ and a cycle period of 2,400s at different elevated temperatures (E2A (220°C, 300°C, and 350°C; E59EG (220°C, 250°C, 300°C, and 350°C; E59S4 (220°C, 350°C). The specimen were fatigued to a certain load cycle number in terms of a fraction of the average live time (N_a -averaged cycle number to failure, $N=0.2 N_a$, $N=0.5N_a$, $N=0.8N_a$, and $N=N_a=800$ cycles). The test then was interrupted for non-destructive tests followed by further fatiguing, etc. The over all result can be presented in micromagnetic life-cycle diagrams as shown exemplarily for instance in case of the measuring quantity K (distortion factor of the tangential field strength, measured according to Fig. 5) in Figure 21.

Concerning the decreasing of K the material states of E2A show the strongest effect compared with the E59EG states in case of the fatigue test temperature of 300°C. The decrease here is stronger than for the test temperature of 350°C. Obviously most of the decrease is in the first fatigue time interval, followed only by a moderate further decreasing, what allows the interpretation that due to strain hardening and dislocation development local precipitation sources are generated enhancing the Cu precipitation. K seems more influenced by the dislocation strengthening effect than by the precipitation what is seen in the secondary fatigue interval. However, very rapidly critical material states are obtained which is documented by the fact that all specimens under these conditions early failed in the following fatigue intervals.

As the first decrease in E2A fatigued at 350°C is smaller compared to the 300°C test the strain hardening effect seems to be smaller, may be, due to recovery effects by transverse dislocation slipping. This is confirmed by measurement of the volume fraction of Cu precipitates performing SANS.

The smallest effects are observed with the stabilised annealed material. As due to this processing most of the Cu content is precipitated in coarse particles the decrease in K is mainly due to fatigue effects (dislocation cell development and cell size change and arrangement) and not due to thermal ageing, i.e. further pronounced precipitation.

The overall 3MA approach, by taking in addition other 3MA-quantities in account and combining these, has used a generic algorithm (Szielasko, 2001) for prediction of the Vickers

hardness 10 and the G- value (Figure 22, Figure 23) with very high confidence level and regression coefficient. The G-value is the electrical residual resistance ratio which is defined as the ratio of the specific resistance measured at ambient temperature to the specific resistance measured at nitrogen temperature. G is a measure of impurity (foreign atoms in the iron matrix) of a material and here therefore is a direct measure of the Cu content of the precipitates. The MPA measures G very carefully in the laboratory and has compared the results with SANS measurements. There is a linear correlation (Figure 24).

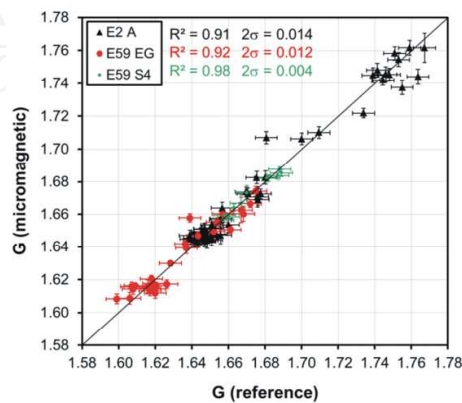


Fig. 22. 3MA prediction of the G-value

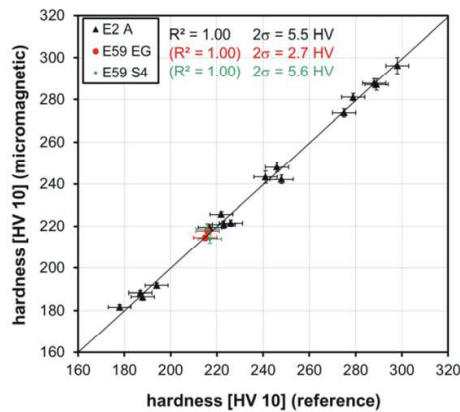


Fig. 23. 3MA prediction of the Vickers hardness 10

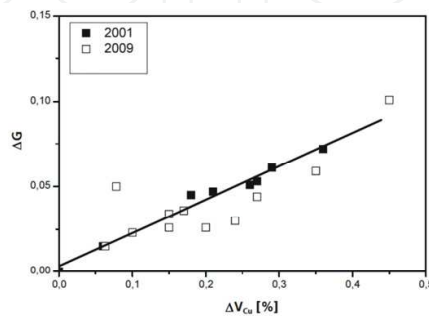


Fig. 24. Change in the G-value (ΔG) compared with the change in Vol.% Cu precipitation (ΔV_{Cu}) determination with SANS (measurements from the years 2001 and 2009)

With 3MA there is therefore a reliable ability to characterise the degradation in terms of the Cu precipitates volume fraction as well as in hardness.

Concerning the expected DSA-effects the investigations have shown serrations in the stress-strain diagrams only in the small temperature window 130-185°C. At service temperature it does not play a role.

4. NDT characterisation of fatigue at austenitic stainless steels

Activities to the non-destructive characterisation of fatigue phenomena at austenitic steels were performed in a co-operation with the Institute of Material Science and Engineering of the Technical University Kaiserslautern, Germany and started in 1999 with 2 PhD thesis's (Bassler, H.J., 1999; Lang M., 1999).

Austenitic steel of the grade AISI 321 (German grade 1.4541 - Ti-stabilised and AISI 347 German grade 1.4550 - Nb-stabilised) is often used in power station and plant constructions. The evaluation of early fatigue damage and thus the remaining lifetime of austenitic steels is a task of enormous practical relevance. Meta-stable austenitic steel forms ferromagnetic martensite due to quasi-static and cyclic loading. This presupposes the exceeding of a threshold value of accumulated plastic strain. The amount of martensite as well as its magnetic properties should provide information about the fatigue damage. Fatigue experiments were carried out at different stress and strain levels at room temperature (RT) and at $T = 300^{\circ}\text{C}$. The characterisation methods included microscopic techniques such as light microscopy, REM, TEM and scanning acoustic microscopy (SAM) as well as magnetic methods, ultrasonic absorption, X-ray and neutron diffraction. Sufficient amounts of mechanical energy due to plastic deformation lead to phase transformation from fcc austenite without diffusion to tetragonal or bcc ferromagnetic α' -martensite. As the martensitic volume fractions are especially low for service-temperatures of about 300°C highly sensitive measuring systems are necessary. Besides systems on the basis of a HT-SQUID (High Temperature Super Conducting Quantum Interference Device) special emphasis was on the use of GMR-sensors (giant magnetoresistors) which have the strong advantage to be sensitive for DC-magnetic fields too without any need for cooling (Yashan, 2008). In combination with an eddy-current transmitting coil and universal eddy-current equipment as a receiver the GMR-sensors were used especially to on-line monitoring the fatigue experiments in the servo-hydraulic fatigue machine.

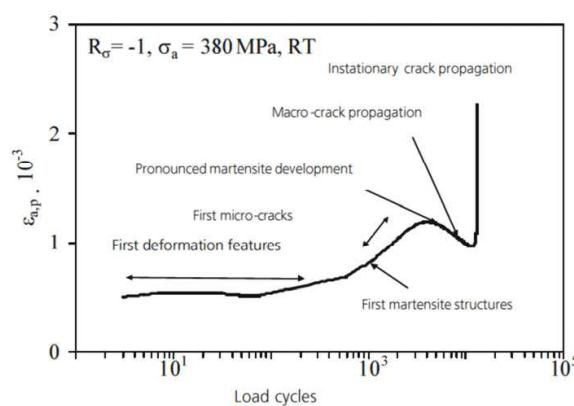


Fig. 25. Fatigue at RT

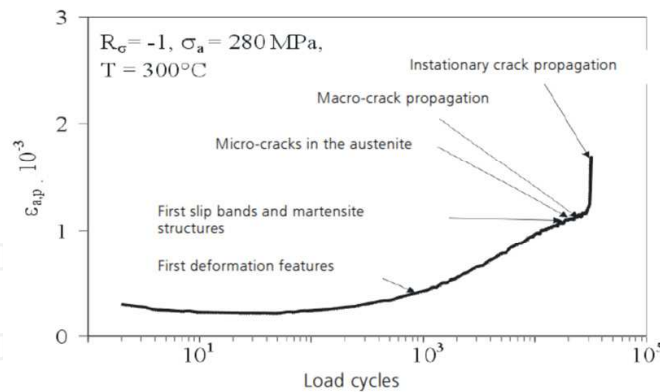


Fig. 26. Fatigue at 300°C

As function of fatigue these steels at room temperature show secondary hardening caused by continuously increasing martensite formation. Martensitic volume fractions created at service temperature $T = 300^{\circ}\text{C}$ are too small to cause cyclic hardening. Generally speaking, an accelerated martensite formation leads to shortened life times in cyclic deformation experiments. At room temperature crack initiation mainly takes place in martensitic regions (besides slip bands in the austenite phase) and often starting at carbonitrides. In martensitic regions a zigzag-shaped crack path is observed causing slower crack propagation. At $T = 300^{\circ}\text{C}$ crack initiation only occurs at slip bands. Increasing martensite formation is an indicator for increasing material damage subsequent to cyclic loading. The detection of martensite at austenitic components can be seen as a hint to local plastic deformation and thus local damage. Figure 25 and Figure 26 show the fatigue damage development and accumulation in the case of the 1.4541 material (Ti stabilised) at RT and at 300°C as can be revealed by optical and electron microscopy as function of the load cycles in cyclic deformation curves. The one-step fatigue test was performed stress controlled and mean stress-free.

By using the GMR as eddy current receiver online and in real time the fatigue experiment was monitored in the servo-hydraulic testing machine. Figure 27 (one-step fatigue tests) and Figure 28 (multiple step loading and load mix) document results obtained during online measurement in real time.

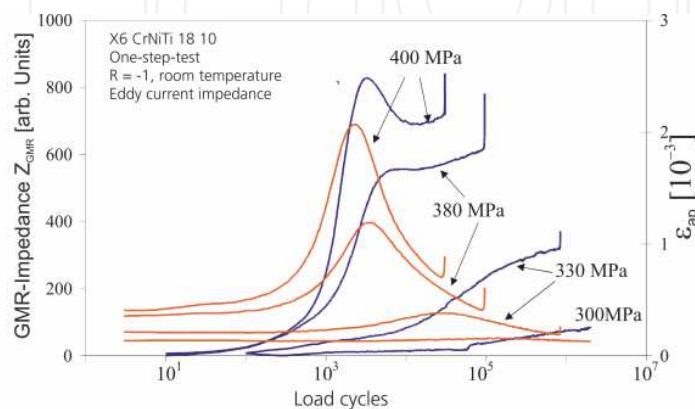


Fig. 27. One-step stress controlled fatigue tests at room temperature

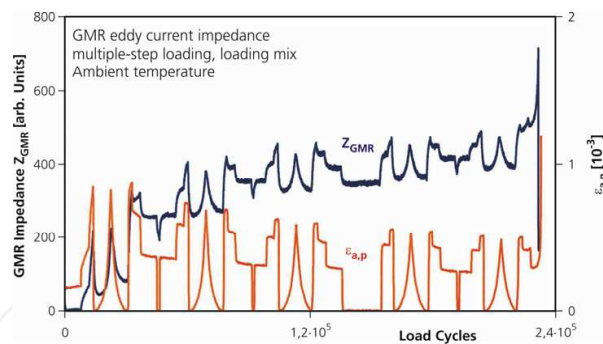


Fig. 28. Multiple step stress controlled fatigue test with time dependent load mix at room temperature

The NDT-quantity measured is the eddy current GMR-transfer impedance (Figure 27) which clearly indicates the fatigue behaviour and gives an early warning before failure. In the case where the secondary hardening effect due to the martensite formation is pronounced (stress > 380MPa) the impedance shows this secondary hardening effect too. In the multiple step experiment the impedance follows exactly the time function of the total strain but with an off-set indicating the martensite development.

It should be mentioned here that these monitoring technique was performed at plain carbon steel too. However, here the measuring effects are one order in magnitude smaller because not phase transformation to martensite takes place and only changes in the dislocation cell structure are to observe in the microstructure.

The online monitoring measuring technique was enhanced at the technical university Kaiserslautern and another type of sensor was integrated by IZFP (Altpeter, I., Tschunky, R., Hällen, K., Dobmann, G., Boller, Ch., Smaga, M., Sorich, A., & Eifler, D., 2011) into the servo-hydraulic machine. Because fatigue experiments should be monitored at service temperature of 300°C the idea was to integrate ultrasonic transducers in the clamping device of the fatigue specimen and to monitor the ultrasonic time-of-flight (tof) of a pulse propagating from the transmitter to the receiver transmitting the fatigue specimen (Figure 29). Because of the high temperature exposition coupling-free electromagnetic acoustic transducers (EMAT) were used based on a pan cake eddy current coil superimposing a normal magnetic field produced by a permanent magnet. By exciting Lorentz forces radially polarized shear waves are excited (Salzburger, 2009).

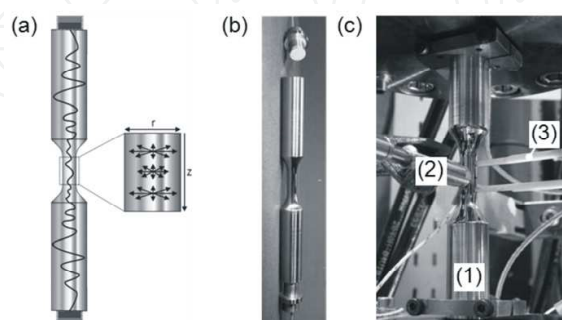


Fig. 29. Schematic diagram of wave propagation: wave propagation direction 'z' and particle displacement 'r' (a), fatigue specimen and EMAT probes with radial polarized wave type (b), clamped fatigue specimens (1) in grips, which enclose the transmitter at the one end and received at the other as well as Ferritescope (2) and an extensometer (3) (c)

The Ferritescope is used at room temperature experiments to measure the content of the developing martensite phase. The material investigated was the meta-stable AISI 347 with low C-content (0.04 weight %) and high Ni-content (10.64 weight %). Because of this fact a martensite phase transformation develops only at room temperature fatigue experiments. The fatigue tests were performed strain controlled, mean strain-free at a cycling frequency of 0.01 Hz with strain amplitudes 0.8, 1.0, 1.2 and 1.6 %. Figure 30 shows the measurement procedure to measure the tof which is determined as an average value between the maximum and minimum value obtained in each cycle (Figure 31).

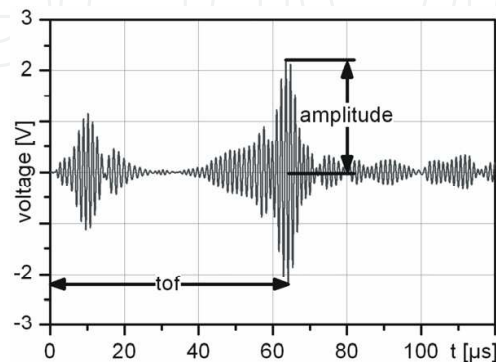


Fig. 30. Time-of-flight (tof) measurement procedure

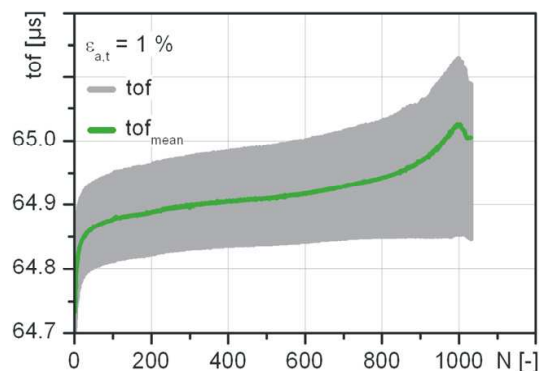


Fig. 31. Determination of the average (mean) tof-value at ambient temperature

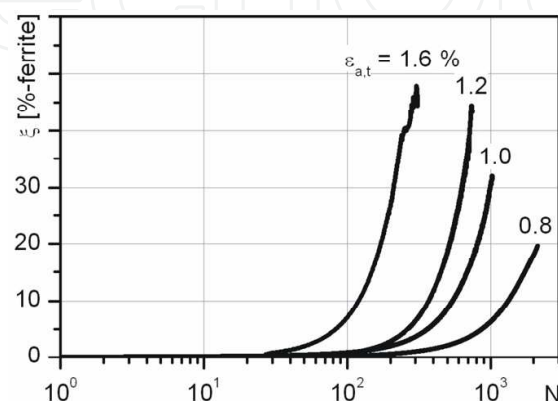


Fig. 32. Cyclic deformation curves at ambient temperature

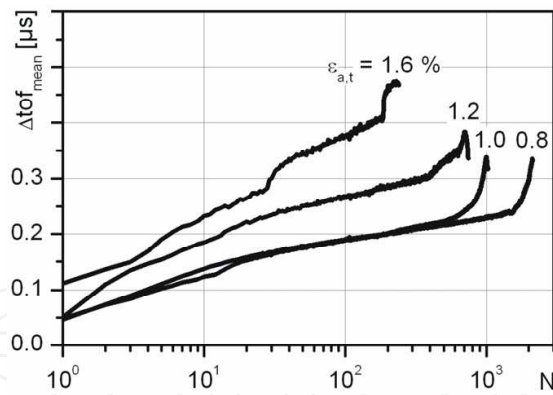


Fig. 33. Mean tof-curves at ambient temperature

The mean tof-value measured online shows a distinct behaviour as function of the fatiguing and is different in the case of ambient temperature and at 300°C. Figure 32 shows the cyclic deformation curves and Figure 33 the respective mean tof-curves where clearly the martensite development can be identified. The behaviour at 300°C is documented in the Figures 34 and Figure 35.

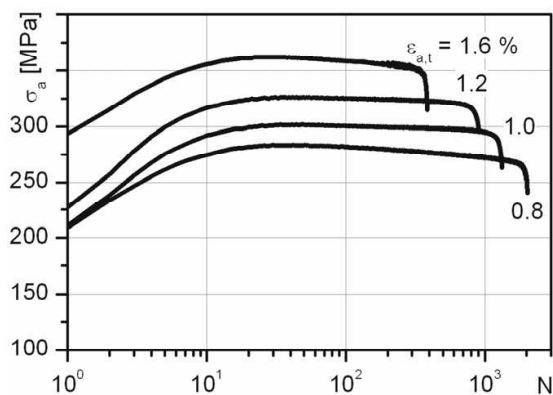


Fig. 34. Cyclic deformation curves at 300°C

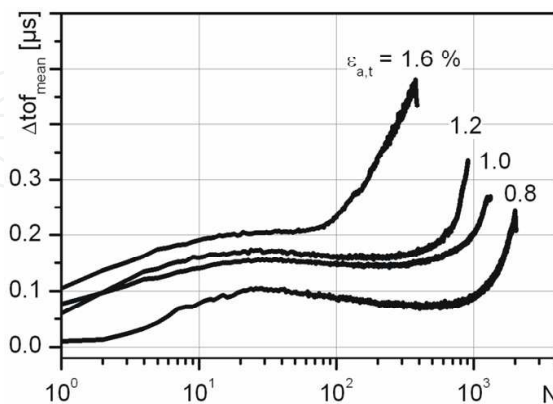


Fig. 35. Behaviour of the mean tof-values at 300°C

For further development of the tof-technique in order to be used for online monitoring of plant components Rayleigh surface waves or shear horizontal waves excited and received by EMATs will be applied.

5. NDT for characterisation of neutron degradation

In the case of power plant components, such as pressure vessels and pipes, the fitness for use under mechanical loads is characterised in terms of the determination of mechanical properties such as mechanical hardness, yield and tensile strength, toughness, shift of Ductile-to-Brittle Transition Temperature (DBTT), fatigue strength. With the exception of hardness tests which are weakly invasive, all of these parameters can be determined within surveillance programs by using destructive tests only on special standardized samples (Charpy V samples and standard tensile test specimens). The specimens are exposed in special radiation chambers near the core of the Nuclear Power Plant (NPP) to a higher neutron flow than at the surface of the pressure vessel wall in order to generate a worst case. From time to time these specimens are removed from the chambers and used for destructive tests. The number of the samples is limited and in the future it will be very important that reliable non-destructive methods are available to determine the mechanical material parameters on these samples without destruction of the specimens. Furthermore an in situ characterisation of the reactor pressure vessel inner wall through the cladding is of interest for inservice inspection, additionally to the measurements on samples.

To solve this task a combination testing technique based on 3MA and the dynamic magnetostriction measurement by using an EMAT (Electromagnetic Acoustic Transducers) was developed.

Sample set of neutron irradiated base material

Material	Short term	Neutron-fluence [n/cm ²]	Range ΔT_{41} [K]
22 NiMoCr 3 7	P7	0 – 5.38 x 10 ¹⁸	0 - 32
20 MnMoNi 5 5	P141	0 – 10.7 x 10 ¹⁸	0 - 9
22 NiMoCr 3 7	P147	0 – 44.0 x 10 ¹⁸	0 - 23
ASTM A508 C1.3 (22 NiMoCr 3 7)	JFL	0 – 86.0 x 10 ¹⁸	0 - 78
ASTM A533B C1.1 (20 MnMoNi 5 5)	JRQ	0 – 98.0 x 10 ¹⁸	0 - 221

Sample set of neutron irradiated weld material

Material	Short term	Neutron-fluence [n/cm ²]	Range ΔT_{41} [K]
S3NiMo3-UP	P16	0 – 11.6 x 10 ¹⁸	0 - 67
S3NiMo1-UP	P141	0 – 13.9 x 10 ¹⁸	0 - 38
S3NiMo1	P140	0 – 10.4 x 10 ¹⁸	0 - 21

Table 1. Material description of investigated Charpy samples, base and weld material

The neutron induced embrittlement results in microstructure changes. These microstructure changes are the generation of vacancies and precipitations of Cu-rich coherent particles (radius: 1-1.5 nm). This results in an increase of yield strength and tensile strength, a decrease of Charpy energy upper shelf value and an increase of DBTT.

The potential of micromagnetic testing methods for detection of Cu-precipitates was demonstrated in chapter 3. The interaction between dislocations and copper particles leads to an increase of mechanical hardness and the interaction of the copper particles and Bloch-walls leads to an increase of magnetic hardness. Since the dynamic magnetostriction is sensitive for lattice defects it was assumed that a magnetostrictively excited standing wave in the pressure vessel wall should reflect the neutron embrittlement too and first experiments were performed with a special designed magnetostrictive transducer at Charpy specimens in the hot cell in order to principally demonstrate the potential.

Using several electromagnetic measurements at the same time, a variety of measuring quantities is derived for each measurement cycle. When combined, they achieve the desired result (e.g. material property) more efficiently compared to individual measurement. By using a calibration function or pattern recognition the desired quantity of an unknown set of samples investigated by that method can be detected non-destructively.

Depending on the specific design of a pressure vessel –which varies in different countries – the pressure vessel material in nuclear power plants is exposed to neutron fluences in the range between 5.6×10^{18} n/cm² and 86.0×10^{18} n/cm². In order to characterise the neutron irradiation-induced embrittlement, Charpy samples exposed to neutron fluence in the above mentioned range have been investigated in a hot cell at AREVA NP whereby only the 3MA and EMAT sensors were arranged within the hot cell and the electronic equipment (3MA and EMAT device) was outside. These Charpy samples (base material and weld material) of Russian and western design have been provided by AREVA NP and the Research Centre Dresden-Rossendorf (see Table 1).

The result of the 3MA-approach based on pattern recognition algorithms are shown in Figure 36 (base material) and Figure 37 (weld material) in terms of changes in the DBTT evaluated at Charpy energy of 41J (ΔT_{41}).

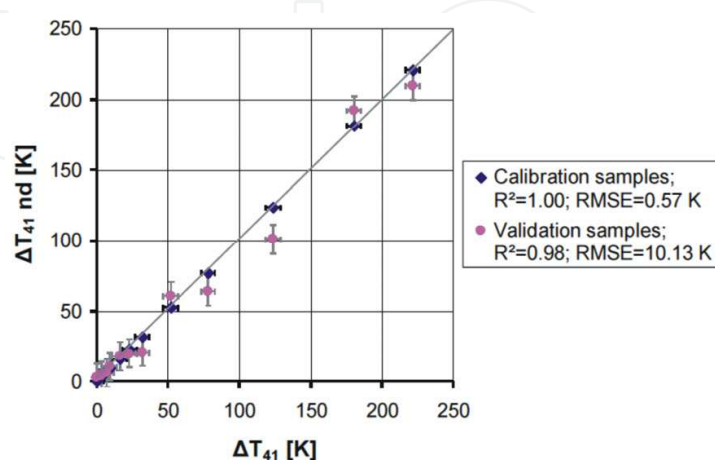


Fig. 36. 3MA prediction of ΔT_{41} in case of the base materials

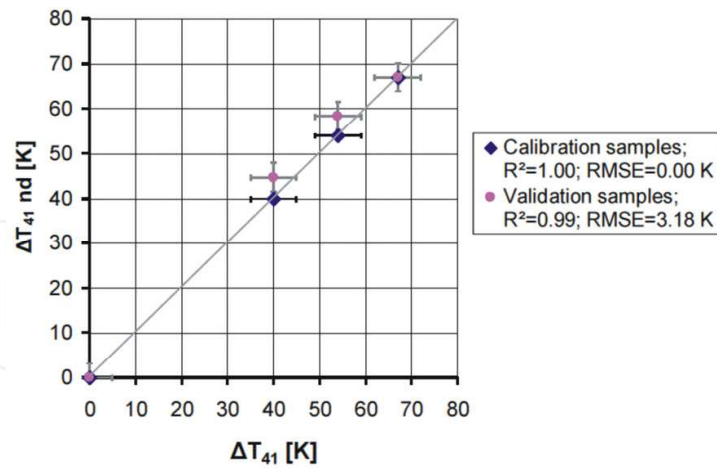


Fig. 37. 3MA prediction of ΔT_{41} in case of weld materials

As can be seen, excellent correlation coefficients on high confidence levels were obtained. Very important in this context is the contribution of the dynamic magnetostriction which is measured as the sensitivity to excite an ultrasonic standing wave in the base material under the cladding in the pressure vessel wall. Here the electrical conductivity and magnetic permeability in the ferritic-martensitic steel structure is higher than in the austenitic cladding and therefore the efficiency to excite eddy currents is enhanced but this region is also the most influenced microstructure by the irradiation.

The enhanced electrical conductivity and permeability facilitate the excitation and the large lift-off effect of the transducer due to the cladding can be compensated by the higher eddy-current density.

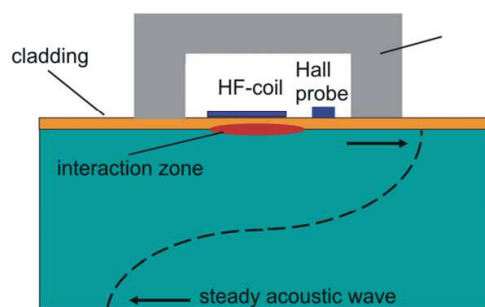


Fig. 38. Magnetostrictively excited standing wave in the PV-wall

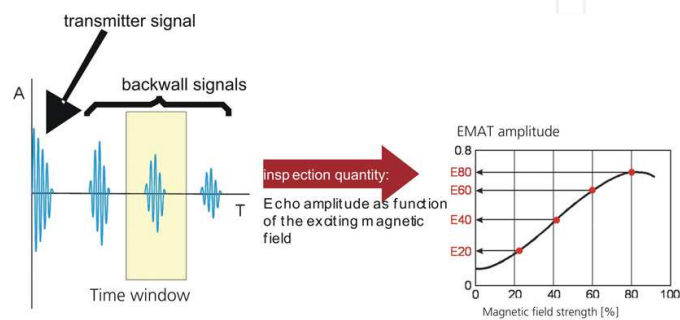


Fig. 39. Inspection quantity selected E60

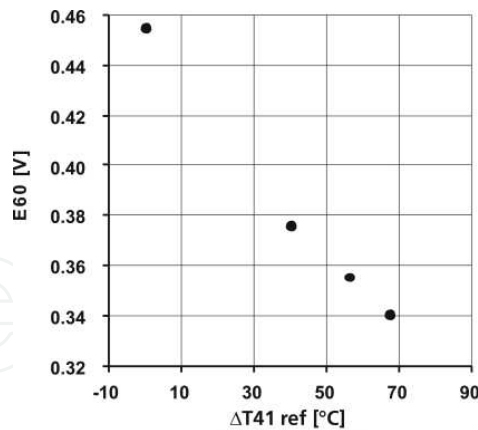


Fig. 40. Correlation of the quantity E60 with the DBTT shift at 41J Charpy energy

Figure 38 shows the measurement principle and Figure 39 defines the measurement quantity E60 which is the dynamic magnetostriction, i.e. the magnetostrictively excited ultrasound amplitude when the transducer is using a magnetic field magnitude which is 60% of the maximum field delivered by the current generator. The linear correlation of E60 with ΔT_{41} is documented in Figure 40.

6. Conclusion

By use of micromagnetic non-destructive techniques the ability to characterise materials ageing was demonstrated, in terms of hardness enhancement and Cu precipitation due to thermal degradation, in terms of supplying an early warning before fatigue life is elapsed due to Low Cycle Fatigue, and in terms of indicating the DBTT 41J shift when material degradation is due to neutron embrittlement. The demonstration was at well defined laboratory-type specimens but a high sensitivity and confidence in the results was obtained.

However, the next development step to perform is the demonstration of the techniques at real life components and the integration in inservice testing respectively in ageing management procedures of real plants. This will in addition include UT by using EMAT.

As the special application of EMAT sensors has demonstrated its reliable use at a service temperature of 300°C the integration of this sensor type into plant lifetime management systems should be an engineering problem which is to solve concerning the proper selection of cooling devices for the driving microelectronic systems and heat resistant wires for coils and cables especially isolated for high temperature access.

An EMAT itself is 'no more' than a magnet-inductive transducer of which the induced eddy current field is superimposed by a magnetic field. The last can be static as well as dynamic. When the superimposed magnetic field is changed dynamically in a hysteresis loop the EMAT can be applied to collect as well other micromagnetic quantities as a combination sensor for 3MA.

One strong critic comes always up when micromagnetic techniques are discussed for materials characterisation. This is the need of defined calibration specimens and the efforts for recalibration when transducers have to be adapted or are to replace after repair. Therefore the scientific community works hard to define and optimise robust calibration procedures to reduce or even to avoid the efforts and first success can be reported.

When material microstructure states are needed for reference to fix absolutely a time scale, for instance in fatigue life estimation, the procedure can be applied always when a component starts into new life, for instance after a replacement.

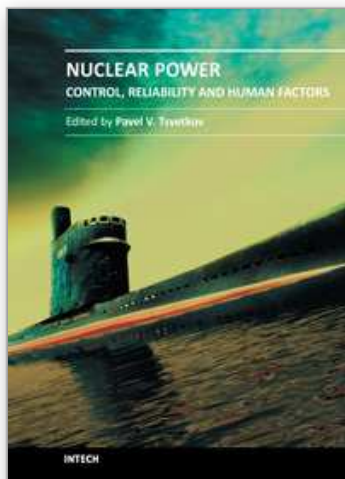
7. Acknowledgment

The author very much acknowledges the high valued contribution of his colleagues from Fraunhofer-IZFP which are Iris Altpeter, Klaus Szielasko, Madalina Rabung, Ralph Tschuncky, Gerhard Hübschen, and Karl Hällen. The special thank is to the Materials Testing Institute, MPA, at the University Stuttgart (Prof. E. Roos) and to the Institute of Material Science and Engineering, WKK, (Prof. D. Eifler) at the Technical University Kaiserslautern with their teams for the long year fruitful co-operation. Last but not least thank is to the ministry of economy and technology for the financial support in different projects beginning in 1979 up to now.

8. References

- Allen, A.J. & Buttle, D.J. (1992). From Microstructural Assessment to Monitoring Component Performance - A Review Relating Different Non-Destructive Studies", *Nondestructive Characterisation of Materials V*, T. Kishi, T. Saito, C. Ruud, R. Green, Eds., Plenum Press, New York, pp. 9 - 30
- Altpeter, I, Dobmann, G., Katerbau K.H., Schick, M., Binkele, P, Kizler, P., & Schmauder, S. (1999). Copper precipitates in the steel 15 NiCuMoNb 5 (WB 36): Material properties and microstructure, atomistic simulation, NDE by micromagnetic techniques, *Proceedings of the 25 MPA Seminar*, 7-8 October, Stuttgart
- Altpeter I. (2002). Electromagnetic and Micro-Magnetic Non-Destructive Characterisation (NDC) for Material Mechanical Property Determination and Prediction in Steel Industry and in Lifetime Extension Strategies of NPP Steel Components, *Inverse Problems*, 18, pp. 1907-1921
- Altpeter, I., Dobmann, G., Kröning, M., & Rabung, M. (2009). Micro-Magnetic Evaluation of Micro Residual Stresses of the IInd and IIIrd Order, *NDT & E International*, 42, 4
- Altpeter, I., K., Szielasko, K., Dobmann, G., Ruoff, H., & Willer, D. (2010), Influences of ageing processes on the fatigue life-time and toughness of the low alloyed steel WB 36, *Report No 090116-TW of the Fraunhofer-IZFP*
- Altpeter, I., Tschuncky, R., Hällen, K., Dobmann, G., Boller, Ch., Smaga, M., Sorich, A., & Eifler, D. (2011). Early detection of damage in thermo-cyclically loaded austenitic materials, submitted for publication in the ENDE 2011 proceedings, *ENDE 2011 conference*, March 10-12, Chennai
- Bassler, H.J. (1999). Cyclic deformation behaviour and plasticity-induced martensite formation of the austenitic stainless steel X6CrNiTi1810, PhD-thesis at the university, Kaiserslautern
- Burkhart, G.L. & Kwun, H. (1989). Measurement of residual stresses around a circular patch weld using Barkhausen noise, *Review of Progress in Quantitative NDE*, Vol. 8B, D. O. Thompson, D. Chimenti, Eds. Plenum Press, New York, p. 2043
- Buttle, D.J. & Hutchings, M.T. (1992). Residual stress measurements at NNDTC, *British Journal of NDT*, Vol. 34, No 4, 175
- Cullity, B.D. (1972). *Introduction to magnetic materials* Addison- Wesley, London
- Fillon, G., Lord, M., & Bussière, J.F. (1990). Coercivity Measurement from Analysis of the Tangential Magnetic Field, *Nondestructive Characterisation of Materials IV*, C. Ruud, J.F. Bussière, R. Green, Eds., Plenum Press, New York, pp. 223 - 230

- Jansky, J., Andrä, T., & Albrecht, K. (1993). Feedwater piping guillotine breaks at 340°C operation temperature, *Transactions of the 12th Intern. Conf. on Structural Mechanics in Reactor Technology*, ed. K.Kussmaul, North-Holland, Vol F, pp. 207-214
- Jiles, D.C. (1988). Review of magnetic methods for nondestructive evaluation, *NDT International*, Vol. 21, 311
- Jiles, D.C. (1990). Microstructure and stress dependence of the magnetic properties of steels, *Review of Progress in Quantitative NDE*, Vol. 9, D. O. Thompson, D. Chimenti, Eds. Plenum Press, New York, p. 1821
- Kneller, E. (1966). *Ferromagnetismus*, Springer, Berlin
- Koch R. & Höller, P. (1989). A modulus for the evaluation of the dynamic magnetostriction as a measured quantity for 3MA, *Nondestructive Characterisation of Materials III*, P.Höller, V. Hauk, G. Dobmann, C. Ruud, R. Green, Eds., Springer, Berlin, p. 644
- Lang, M. (1999). Non-destructive characterisation of the cyclic deformation behaviour and plasticity-induced martensite formation of the austenitic stainless steel X6CrNiTi1810 by sensitive magnetic sensors, PhD-thesis at the Saarland University, Saarbrücken
- Matzkanin, G.A., Beissner, R.E. & Teller, E.M. (1979). *The Barkhausen Effect and its Application to Nondestructive Evaluation*, NTIAC report 79-2, pp 1-49, Nondestructive Testing Information Analysis Center, San Antonio, Texas
- McClure, J.C. & Schröder, K. (1976). The Barkhausen effect. *Critical Reviews in Solid State Sciences*, 6, 45
- Pitsch, H. (1989). Die Entwicklung und Erprobung der Oberwellenanalyse der magnetischen Tangentialfeldstärke als neues Modul des 3MA-Ansatzes, PhD-Thesis, Saarland University, Saarbrücken
- Rabung, M. (2004). Erarbeitung metallphysikalischer Grundlagen zur Anwendung der Mikromagnetik zum Nachweis der Werkstoffveränderungen infolge von Kupfereinscheidungen. PhD Thesis, Saarland University, Saarbrücken
- Sablik, M.J., Burkhart, G.L., Kwun, H., & Jiles, D.C. (1988). A model for the effect of stress on the low-frequency harmonic content of the magnetic induction in ferromagnetic materials. *J. Appl. Phys.* 63, 3930
- Salzburger, H.J. (2009). H.J. EMATs and its Potential for Modern NDE - State of the Art and Latest Applications, *proceedings of the IEEE International Ultrasonics Symposium 1*, 621-628
- Seeger, A. (1966), *Moderne Probleme der Metallphysik*, Springer, Berlin
- Solomon, H.D. & De Lair, A.E. (2001). The influence of dynamic strain ageing on the low cycle fatigue behaviour of low alloyed and carbon steels in high temperature water, *General Electric Research and Development Centre, Technical Information Series, CRD 134*
- Szielasko, K. (2000). Aufbau eines Modulare Messsystems auf Softwarebasis zur Zerstörungsfreien Charakterisierung des Versprödungszustandes von kupferhaltigen Stählen. Diplomarbeit. Hochschule für Technik und Wirtschaft des Saarlandes, Saarbrücken
- Theiner W.A., & Waschkes E. (1984). Method for the non-destructive determination of material states by use of the Barkhausen-effect, Patent DE 2837733C2
- Theiner, W.A., Altpeter, I., & Reimringer, B (1989), The 3MA-testing equipment, application possibilities and experiences, *Nondestructive Characterisation of Materials III*, P.Höller, V. Hauk, G. Dobmann, C. Ruud, R. Green, Eds., Springer, Berlin, p. 699
- Yashan, A. (2008). Über die Wirbelstromprüfung und magnetische Streuflussprüfung mittels GMR-Sensoren, PhD-thesis at the Saarland University, Saarbrücken



Nuclear Power - Control, Reliability and Human Factors

Edited by Dr. Pavel Tsvetkov

ISBN 978-953-307-599-0

Hard cover, 428 pages

Publisher InTech

Published online 26, September, 2011

Published in print edition September, 2011

Advances in reactor designs, materials and human-machine interfaces guarantee safety and reliability of emerging reactor technologies, eliminating possibilities for high-consequence human errors as those which have occurred in the past. New instrumentation and control technologies based in digital systems, novel sensors and measurement approaches facilitate safety, reliability and economic competitiveness of nuclear power options. Autonomous operation scenarios are becoming increasingly popular to consider for small modular systems. This book belongs to a series of books on nuclear power published by InTech. It consists of four major sections and contains twenty-one chapters on topics from key subject areas pertinent to instrumentation and control, operation reliability, system aging and human-machine interfaces. The book targets a broad potential readership group - students, researchers and specialists in the field - who are interested in learning about nuclear power.

How to reference

In order to correctly reference this scholarly work, feel free to copy and paste the following:

Gerd Dobmann (2011). Non-Destructive Testing for Ageing Management of Nuclear Power Components, Nuclear Power - Control, Reliability and Human Factors, Dr. Pavel Tsvetkov (Ed.), ISBN: 978-953-307-599-0, InTech, Available from: <http://www.intechopen.com/books/nuclear-power-control-reliability-and-human-factors/non-destructive-testing-for-ageing-management-of-nuclear-power-components>

INTECH
open science | open minds

InTech Europe

University Campus STeP Ri
Slavka Krautzeka 83/A
51000 Rijeka, Croatia
Phone: +385 (51) 770 447
Fax: +385 (51) 686 166
www.intechopen.com

InTech China

Unit 405, Office Block, Hotel Equatorial Shanghai
No.65, Yan An Road (West), Shanghai, 200040, China
中国上海市延安西路65号上海国际贵都大饭店办公楼405单元
Phone: +86-21-62489820
Fax: +86-21-62489821

© 2011 The Author(s). Licensee IntechOpen. This chapter is distributed under the terms of the [Creative Commons Attribution-NonCommercial-ShareAlike-3.0 License](#), which permits use, distribution and reproduction for non-commercial purposes, provided the original is properly cited and derivative works building on this content are distributed under the same license.

IntechOpen

IntechOpen